

Proposal for III-V ordered alloys with infrared band gaps

Su-Huai Wei and Alex Zunger

Citation: *Applied Physics Letters* **58**, 2684 (1991); doi: 10.1063/1.104807

View online: <http://dx.doi.org/10.1063/1.104807>

View Table of Contents: <http://scitation.aip.org/content/aip/journal/apl/58/23?ver=pdfcov>

Published by the AIP Publishing

Articles you may be interested in

[Interpolating semiconductor alloy parameters: Application to quaternary III-V band gaps](#)

J. Appl. Phys. **94**, 5814 (2003); 10.1063/1.1613371

[Near band edge absorption spectra of narrow-gap III-V semiconductor alloys](#)

J. Appl. Phys. **80**, 4045 (1996); 10.1063/1.363364

[Atomic ordering in III/V semiconductor alloys](#)

J. Vac. Sci. Technol. B **9**, 2182 (1991); 10.1116/1.585761

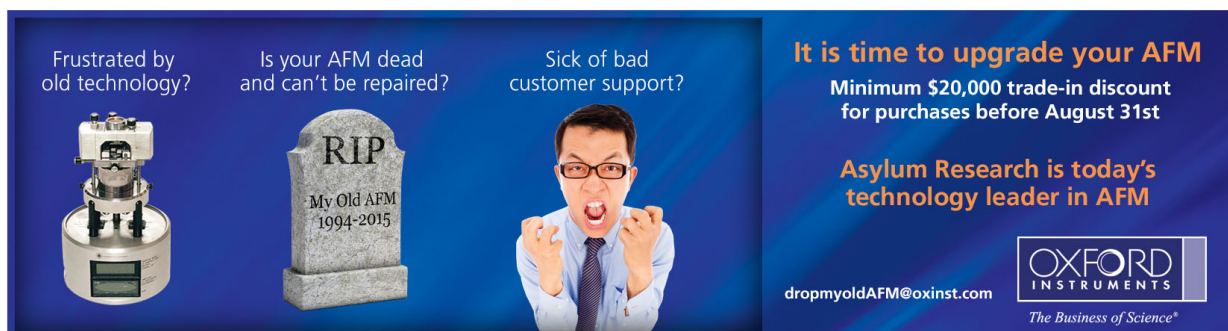
[Band-gap narrowing in novel III-V semiconductors](#)

J. Appl. Phys. **68**, 3747 (1990); 10.1063/1.346291

[Effect of mismatch strain on band gap in III-V semiconductors](#)

J. Appl. Phys. **57**, 5428 (1985); 10.1063/1.334817

Frustrated by old technology? Is your AFM dead and can't be repaired? Sick of bad customer support?



It is time to upgrade your AFM
Minimum \$20,000 trade-in discount
for purchases before August 31st

**Asylum Research is today's
technology leader in AFM**

**OXFORD
INSTRUMENTS**
The Business of Science®

dropmyoldAFM@oxinst.com

Proposal for III-V ordered alloys with infrared band gaps

Su-Huai Wei and Alex Zunger

Solar Energy Research Institute, Golden, Colorado 80401

(Received 21 February 1991; accepted for publication 5 April 1991)

It is shown theoretically that the recently observed spontaneous ordering of III-V alloys that yields alternate monolayer (111) superlattices provides the opportunity for achieving infrared band gaps in systems such as $(\text{InAs})_1(\text{InSb})_1$ and $(\text{GaSb})_1(\text{InSb})_1$. A substantial reduction in the *direct* band gap is predicted to result from the *L*-point folding that repel the Γ band-edge states.

Substantial effort has recently been focused on developing semiconductor materials for infrared (IR) devices in the wavelength range¹ above 8 μm . In addition to the use of intersubband absorption in tunnelling III-V superlattices,² four general physical principles have been previously utilized to directly shift band gaps into the IR spectral range.

(i) *Bulk alloying*. In this simple approach one uses the fact that alloy band gaps vary smoothly and continuously with composition (often with a parabolic deviation from linearity), and seeks a combination of mutually soluble "small gap" SG (e.g., HgTe) and "large gap" LG (e.g., CdTe) semiconductors that produces a $(\text{SG})_{1-x}(\text{LG})_x$ alloy with a desired IR gap.

(ii) *Superlattice quantum confinement without strain*. The basic idea here is to take a semiconductor with a very small gap (SG) and layer it in a $(\text{SG})_p/(\text{LG})_q$ superlattice geometry with a *lattice-matched* material having a larger gap (LG). For small layer thicknesses (p, q), quantum confinement acts to lower the valence-band maximum (VBM) and raise the conduction-band minimum (CBM), thus increasing the superlattice gap above that of pure SG. This was proposed theoretically for SG = HgTe and LG = CdTe by Schulman and McGill³ and by Smith *et al.*⁴ and examined experimentally, e.g., by Reno and Faurie.⁵

(iii) *Superlattice strain-induced band-gap reduction*. The basic idea here is to take a material with a small band gap and small lattice constant (SGSL) and layer it coherently with a material having a larger gap and larger lattice constant (LGLL), forming a strained-layer $(\text{SGSL})_p/(\text{LGLL})_q$ superlattice. Coherence of SGSL with LGLL then *expands* the lattice constant of SGSL parallel to the interface, thus lowering its Γ conduction-band minimum. At the same time, tetragonal *compression* of SGSL in the perpendicular direction splits its VBM, raising the energy of the upper split components. Both effects act to reduce the band gap relative to unstrained bulk SGSL. This approach has been proposed by Osbourn⁶ for $\text{SGSL} = \text{InAs}_{0.39}\text{Sb}_{0.61}$ and $\text{LGLL} = \text{InAs}_{1-x}\text{Sb}_x$ with $x > 0.61$. Since quantum confinement effects at small (p, q) act in the opposite direction, increasing the band gap, relatively thick layers are needed to achieve the maximum band-gap narrowing.^{6,7} Yet, the need to accommodate coherently the misfit strain limits the maximum thickness that can be used.

(iv) *Superlattice-induced band inversion*. The basic idea here is to form a superlattice in which the CBM of one

of the constituents (AC) is lower in energy than the VBM of the other (BC); in this type of band lineup, the superlattice can have a smaller band gap than either of its constituents. This approach has been proposed by Arch *et al.*⁸ for AC = InAs and BC = GaSb. Like in (iii) above, here, too, relatively thick layer would be required to counteract the quantum confinement effects. However, in such a "type II" band arrangement, thick layers deteriorate severely the intensity of optical absorption due to increased separation between electrons and holes. To reduce the layer thickness needed, the principle of "strain-induced band-gap reduction" [item (iii) above] has been proposed by Smith and Mailhot⁹ for AC = InAs and BC = $\text{Ga}_{1-x}\text{In}_x\text{Sb}$. This system was grown successfully by Chow *et al.*¹⁰ where far-infrared photoluminescence was observed.

We discuss here a different principle of achieving infrared band gaps with III-V materials, namely, "ordering-induced band-gap narrowing." The basic idea is to replace medium thickness⁴⁻¹⁰ by alternate monolayer (111) superlattices, in which the *L* point (rather than the *X* point) folds into the Brillouin zone center. This leads to a repulsion¹¹ of the Γ -like band-edge states that dramatically

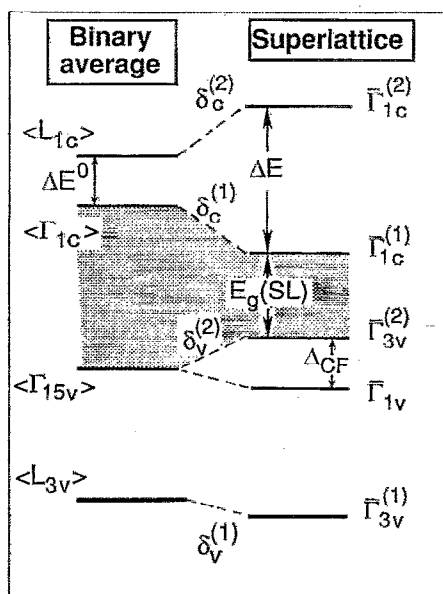


FIG. 1. Schematic plot of energy level shift at $\bar{\Gamma}$ of a typical III-V alloy forming CuPt-like structure. States with same symmetry in the superlattice are of mixed zincblende characters.

TABLE I. Calculated energy differences (eV) between the repelling states $\langle L_{1c} \rangle$ and $\langle \Gamma_{1c} \rangle$ before (ΔE^0) and after (ΔE) the perturbation potential is turned on. Values in parenthesis are for unrelaxed structures.

	GaAs/InAs	GaAs/InSb	GaAs/GaSb	InAs/InSb
$\Delta E^0 = \langle L_{1c} \rangle - \langle \Gamma_{1c} \rangle$	0.99	0.68	0.47	1.0
$\Delta E = \overline{\Gamma}_{1c}^{(2)} - \overline{\Gamma}_{1c}^{(1)}$	1.43 (1.22)	1.22 (1.02)	1.77 (1.28)	1.84 (1.39)
$R = \Delta E - \Delta E^0$	0.44 (0.23)	0.54 (0.34)	1.30 (0.81)	0.84 (0.39)

reduces the direct band gap, thus overwhelming the opposite effect of quantum confinement. The fact that such “natural superlattices” (see below) are ultrathin ($p=q=1$) obviates the difficulties with misfit dislocations and with separation of electron and hole states in type-II systems.

It has recently been noted¹² that numerous III-V alloys exhibit in vapor phase growth *spontaneous* long-range ordering in the form of monolayer (AC)₁/(BC)₁ superlattices in the (111) orientation (the “CuPt-like structure”). The degree of ordering is never perfect; it can however, be maximized in certain growth temperature ranges and substrate misorientations.^{12,13} Examples for observations of CuPt ordering are given in Ref. 12. In all cases, ordering occurred as a result of *homogeneous* alloy growth *without* sequential (shutter-controlled) exposures. Denoting superlattice (SL) states by an overbar and the homogeneous alloy states by angular brackets, folding relations¹¹ show that in a monolayer (111) superlattice the states at the $\overline{\Gamma}$ point are constructed from the zincblende-like states at $\langle \Gamma \rangle + \langle L^{111} \rangle$. The folded zincblende states at this wave vector are coupled in the superlattice by the perturbing potential $\delta V(\mathbf{r}) = \delta V^{(\text{chem})} + \delta V^{(\text{size})}$ that has the symmetry of the ternary superstructure. It has a contribution $\delta V^{(\text{chem})}$ due to the chemical disparity between the two mixed atoms and a contribution $\delta V^{(\text{size})}$ arising from their size mismatch. This potential couples the alloy states and leads to a “level repulsion” between them, whereby superlattice states are displaced relative to the unperturbed (virtual crystal) states. For example, the $\overline{\Gamma}$ -folding alloy states $\langle \Gamma_{1c} \rangle$ and $\langle L_{1c} \rangle$ couple through δV , producing the superlattice states $\overline{\Gamma}_{1c}^{(1)}$ and $\overline{\Gamma}_{1c}^{(2)}$ that are lowered and raised, respectively, relative to the averaged alloy states (Fig. 1). The lowering of the CBM will be denoted (Fig. 1) as $\delta_c^{(1)} = \epsilon \langle \Gamma_{1c} \rangle - \epsilon(\overline{\Gamma}_{1c}^{(1)})$, with a similar expression $\delta_c^{(2)} = -\epsilon \langle L_{1c} \rangle + \epsilon(\overline{\Gamma}_{1c}^{(2)})$ for the higher conduction band. Similarly, the alloy valence-band states $\langle L_{3v} \rangle$ and $\langle \Gamma_{15v} \rangle$ produce the superlattice states $\overline{\Gamma}_{3v}^{(1)}$ and $\overline{\Gamma}_{3v}^{(2)}$ that are also mutually repelled (Fig. 1). The increase in the energy of the VBM will be denoted (Fig. 1) as $\delta_v^{(2)} = -\epsilon \langle \Gamma_{15v} \rangle + \epsilon(\overline{\Gamma}_{3v}^{(2)})$. The downward displacement of the $\overline{\Gamma}_{3v}^{(1)}$ (the CBM) and the upward displacement of the $\overline{\Gamma}_{3v}^{(2)}$ (the VBM) reduce the band gap. Figure 1 shows schematically the coupling states at $\overline{\Gamma}$. Since the conduction-band minimum at \overline{X} is considerably higher in these systems¹⁴ than $\overline{\Gamma}_{1c}^{(1)}$, the former will not be discussed here.

To quantify the extent of level repulsion, we denote by ΔE^0 the $\langle L_{1c} \rangle - \langle \Gamma_{1c} \rangle$ energy difference *before* coupling (each term being approximated here and in Table I by the average over the binary constituents calculated at the SL lattice constant), and by ΔE the appropriate energy differ-

ence between the superlattice states $\overline{\Gamma}_{1c}^{(2)}$ and $\overline{\Gamma}_{1c}^{(1)}$. Table I shows ΔE , ΔE^0 and their difference $R = \Delta E - \Delta E^0 = \delta_c^{(1)} + \delta_c^{(2)}$ for four systems, as obtained from the self-consistent band-structure calculations for the CuPt-type superlattices. These were calculated in the local density approximation (LDA), as implemented by the semirelativistic linearized augmented plane-wave (LAPW) method.¹⁵ In all cases we have assumed that the superlattice is matched to a substrate whose lattice constant is the average of its constituents. Table I reveals a substantial conduction-band repulsion R and that the structural piece $\delta V^{(\text{size})}$ of the perturbing potential has a significant contribution to R . This can be exemplified by the results for

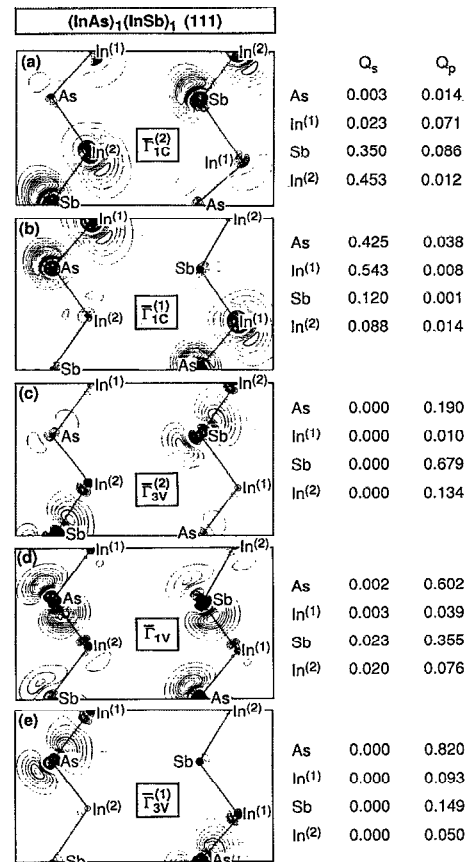


FIG. 2. Wave function amplitudes $|\psi_i|^2$ at the $\overline{\Gamma}$ band-edge states of (InAs)₁(InSb)₁ in CuPt-like structure, plotted in the (110) plane. The contour step size is $4 \times 10^{-3} e/\text{au}^3$. Charges are normalized to $2e/\text{cell}$. On the right-hand side we also give the angular momentum and site decomposed charge (in units of e) for these states, where In⁽¹⁾ and In⁽²⁾ denote In atoms surrounded locally by the As₃Sb and AsSb₃ tetrahedra, respectively.

TABLE II. Experimental low-temperature (LT) band gaps for the binary constituents and our predicted semirelativistic LDA-corrected low-temperature direct band gaps [Eq. (4)] for the four systems forming CuPt-like structure. The numbers in parenthesis are crystal field (denoted Δ_{CF} in Fig. 1) averaged values. The last row gives the change in the spin-orbit splitting $\delta\Delta_0$ relative to their respective averaged binary values. To include spin-orbit interactions, subtract $1/3 \delta\Delta_0$ from $E_g(\text{SL})$. All energies are in eV.

	GaAs/InAs	GaSb/InSb	GaAs/InSb	InAs/InSb
$E_g(\text{binary})^a$	1.52/0.42	0.81/0.24	1.52/0.81	0.42/0.24
$E_g(\text{SL})^b$	0.55 (0.58)	0.09 (0.12)	0.27 (0.36)	-0.28 (-0.20)
$\delta\Delta_0$	-0.01	-0.01	0.08	0.08

^aLow-temperature experimental values, Ref. 16.

^bPredicted low-temperature values at $\bar{\Gamma}$.

InAs/InSb: we find that without structural relaxation [where $\delta V(r) = \delta V^{(\text{chem})}(r)$] band coupling gives $R = 0.39$ eV, while after relaxation $\delta V^{(\text{size})}(r)$ further increases R by an additional 0.45 eV.

Level repulsion also causes mixing and localization of the various states, as illustrated in Fig. 2 for (InAs)₁/(InSb)₁. We see that each member of a pair of coupling states ($\bar{\Gamma}_{3v}^{(1)} + \bar{\Gamma}_{3v}^{(2)}$, or $\bar{\Gamma}_{1c}^{(1)} + \bar{\Gamma}_{1c}^{(2)}$) has its charge localized on a *different* sublattice. For example, the $\bar{\Gamma}_{3v}^{(1)}$ and $\bar{\Gamma}_{1c}^{(1)}$ wave functions are localized on the In—As bonds, whereas the $\bar{\Gamma}_{3v}^{(2)}$ and $\bar{\Gamma}_{1c}^{(2)}$ wave functions are localized on the In—Sb bonds. For the four systems studied here, the valence-band maximum $\bar{\Gamma}_{3v}^{(2)}$ is found to be localized systematically on the heavy atom semiconductor, while the conduction-band minimum $\bar{\Gamma}_{1c}^{(1)}$ is always localized on the light atom partner. Despite this preferred localization the strength of the VBM—CBM optical transition is predicted to be similar to that in the binary constituents,¹⁴ since the SL repeat period is very short. We find that relaxation enhances substantially both the wave function localization and the mixing of *s* character into the valence-band-edge states [Fig. 2(d)] that are pure *p* states in the cubic binary constituents. This affects the spin-orbit splitting Δ_0 .¹¹ Our predicted changes in the spin-orbit splitting $\delta\Delta_0 = \Delta_0[(AC)_1(BC)_1] - 1/2 \Delta_0(AC) - 1/2 \Delta_0(BC)$ are given in Table II. It shows that in the common-anion systems $\delta\Delta_0 \lesssim 0$, while for common-cation systems the negative bowing ($\delta\Delta_0 > 0$) is sizable.

To avoid systematic errors in the LDA-calculated absolute values of the SL band gaps,¹¹ we construct a “predicted SL gap” $E_g(\text{SL})$ by subtracting the calculated level shifts (Fig. 1) from the experimental¹⁶ (exptl) average of the gaps of the *constituents*

$$E_g(\text{SL}) = \{\epsilon\langle\Gamma_{1c}\rangle - \epsilon\langle\Gamma_{15v}\rangle\}_{\text{exptl}} - (\delta_c^{(1)} + \delta_v^{(2)}). \quad (1)$$

This procedure eliminates the LDA errors to first order.¹¹ The predicted band gaps (with ± 0.05 eV uncertainty) are given in Table II.¹⁶ Note that in all systems studied here, the semiconductor partner with the smaller band gap has a *larger* lattice constant than the other partner. Consideration of strain and quantum confinement discussed in item (iii) above would therefore suggest that these SL’s will have a larger band gap than the bulk constituent with the small gap. Table II shows, however, that in all cases except GaAs/InAs the opposite is true: intervalley mixing leads to strong level repulsion that overwhelms other effects. The level repulsion is also larger for systems with smaller en-

ergy denominators¹¹ ΔE^0 (Table I), consistent with a perturbation theory description. Indeed, since the L_{1c} level is closer in most alloys to Γ_{1c} than is X_{1c} , the level repulsion R in (111) SL’s is larger than in (001) SL’s (where Γ couples to X).

Our semirelativistic calculations predict that in the perfectly ordered CuPt-like structure (GaSb)₁/(InSb)₁ and (InAs)₁/(InSb)₁ will have direct band gaps of 0.09 and -0.28 eV, respectively. The band gap will be larger if the systems are not perfectly ordered.¹³ For example, for (InAs)₁(InSb)₁ the band gap could vary from -0.28 eV (fully ordered) to 0.18 eV (random alloy¹⁷). Hence, for a given composition x one has additional control over the band gap through variations of the growth parameters that produce ordering.¹³ Experimental examination of the optical and structural properties of these materials is called for.

This work was supported in part by the U.S. Department of Energy, under grant No. DE-AC02-77-CH00178.

¹See reviews by R. Triboulet, *Semicond. Sci. Technol.* **5**, 1073 (1990) and in *Materials for Infrared Detectors and Sources*, edited by R. F. C. R. Farrow, J. F. Schetzina, and J. T. Cheung (Materials Research Society, Pittsburgh, 1987), Vol. 90.

²B. F. Levine, C. G. Bethea, G. Hasnain, V. O. Shen, E. Pelve, and R. R. Abbott, *Appl. Phys. Lett.* **56**, 851 (1990).

³J. N. Schulman and T. C. McGill, *Appl. Phys. Lett.* **34**, 663 (1979).

⁴D. L. Smith, T. C. McGill, and J. N. Schulman, *Appl. Phys. Lett.* **43**, 180 (1983).

⁵J. Reno and J. P. Faurie, *Appl. Phys. Lett.* **49**, 409 (1986).

⁶G. C. Osbourn, *J. Vac. Sci. Technol. B* **2**, 176 (1984).

⁷S. R. Kurtz, G. C. Osbourn, R. M. Biefeld, L. R. Dawson, and H. J. Stein, *Appl. Phys. Lett.* **52**, 831 (1988).

⁸D. K. Arch, G. Wicks, T. Tonaue, and J.-L. Staudenmann, *J. Appl. Phys.* **58**, 3933 (1985).

⁹D. L. Smith and C. Mailhot, *J. Appl. Phys.* **62**, 2545 (1987); C. Mailhot and D. L. Smith, *J. Vac. Sci. Technol. A* **7**, 445 (1989).

¹⁰D. H. Chow, R. H. Miles, J. R. Soderstrom, and T. C. McGill, *J. Vac. Sci. Technol. B* **8**, 710 (1990).

¹¹S.-H. Wei and A. Zunger, *Appl. Phys. Lett.* **56**, 662 (1990); *Phys. Rev. B* **39**, 3279 (1989).

¹²Literature on ordering in III-V semiconductors is cited in A. Zunger and D. M. Wood, *J. Cryst. Growth* **98**, 1 (1989). See also Ref. 11.

¹³B. T. McDermott, K. G. Reid, N. A. El-Masry, S. M. Bedair, W. M. Duncan, X. Yin, and F. H. Pollak, *Appl. Phys. Lett.* **56**, 1172 (1990).

¹⁴R. G. Dandrea and A. Zunger, *Appl. Phys. Lett.* **57**, 1031 (1990).

¹⁵S.-H. Wei and H. Krakauer, *Phys. Rev. Lett.* **55**, 1200 (1985).

¹⁶*Landolt-Bornstein: Numerical Data and Functional Relationships in Science and Technology*, edited by O. Madelung, M. Schulz, and H. Weiss (Springer, Berlin, 1982), Vol. 17a.

¹⁷The band gap of a random (R) InAs_{0.5}Sb_{0.5} alloy is estimated using the formula $E_g(R) = \bar{E}_g - 1/4b$, where \bar{E}_g is the averaged band gap of the binary constituents (Table II) and $b \approx 0.6$ eV (Ref. 16) is the bowing parameter.